Some Wind and Instability Parameters Associated With Strong and Violent Tornadoes
2. Variations in the Combinations of Wind and Instability Parameters

ROBERT H. JOHNS, JONATHAN M. DAVIES,[1] AND PRESTON W. LEFTWICH

National Weather Service, NOAA, National Severe Storms Forecast Center, Kansas City, Missouri 64106

1. INTRODUCTION

Meteorologists have long known that both potential buoyant energy and the strength and vertical profile of the tropospheric wind fields are important in the process of tornado development [e.g., *Miller*, 1972]. Further, operational experience suggests that the combinations of wind parameters and instability parameters vary considerably from one tornado situation to another. Numerical models suggest that the type of storm that develops in a given situation (e.g., an isolated supercell) is related to both the vertical wind profile and the potential buoyant energy of the air in the updraft entrainment layer [*Weisman and Klemp*, 1982, 1986]. Observational studies by *Rasmussen and Wilhelmson* [1983] and *Leftwich and Wu* [1988] have examined the wind shear/potential buoyant energy relationship in association with tornado development. These studies involved limited data sets and were concerned with the wind shear in a relatively deep layer of the troposphere (0- 4-km above ground level (AGL)). Recently, interest has focused on the nature of the wind fields in shallower layers of the lower troposphere, layers that more nearly correspond to the updraft entrainment region [*Davies*, 1989; *Davies-Jones et al.*, 1990]. Utilizing a large comprehensive data set, *Johns et al.* [1990] (hereafter referred to as JDL) examined the relationship between 0- 2-km AGL "positive" wind shear (PWS) and convective available potential energy (CAPE) [*Moncrieff and Green*, 1972] in association with strong and violent tornado development. In this paper (part 2) the authors review the initial work of JDL and examine additional wind and potential buoyant energy parameter relationships associated with the data set compiled by JDL.

Positive wind shear (PWS), helicity, and deep tropospheric mean wind shear (U) [see *Weisman and Klemp*, 1982] are the three wind parameters with which the relationship with instability is examined. The wind parameters are defined and the method of calculation is discussed in part 1 [*Davies and Johns*, this volume]. The primary instability parameter examined in this study is CAPE. Surface parcel lifted index (SPLI) values based on lifted surface parcel temperatures [*Hales and Doswell*, 1982; *Bothwell*, 1988] are also examined since the SPLI is widely utilized operationally.

2. DETERMINATION OF BUOYANT ENERGY PARAMETER VALUES

2.1. *Calculation of CAPE*

Values of potential buoyant energy for soundings utilized in this study have been determined by an algorithm described by *Doswell et al.* [1982]. The values are essentially equivalent to CAPE with the lifted layer being the lowest 100 mbar AGL. To make representative estimates of CAPE in the vicinity of events considered for inclusion in the data set, these guidelines were followed:

1. If a tornado case occurred within $1\frac{1}{2}$ hours of the sounding time, within 40 nautical miles (74 km) of the sounding site, and in the same air mass as the sounding site, the CAPE value from the sounding was used directly.

2. For tornado cases not satisfying the conditions in guideline 1, the thermodynamic profiles of the surrounding soundings were examined. Interpolation of a CAPE value for both the time and location of the tornado event from the CAPE values computed for the regularly scheduled soundings was attempted only if (1) the horizontal temperature gradients at the standard levels above the boundary layer appeared to be relatively weak and (2) surface data and the temperature and moisture stratification in the boundary layer of the soundings indicated that any instability maximum (center or axis) associated with the case was adequately sampled by at least two nearby stations.

[1]Also at Davies, Incorporated, Pratt, Kansas 67124.

The Tornado: Its Structure, Dynamics, Prediction, and Hazards.
Geophysical Monograph 79

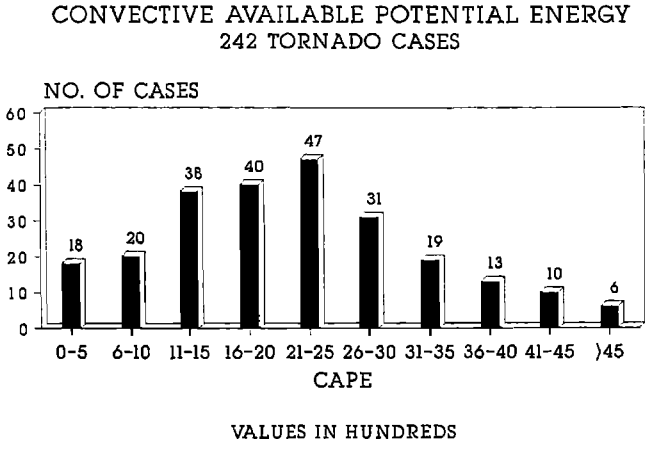

Fig. 1. Distribution of the convective available potential energy (CAPE) values associated with the 242 strong and violent tornado cases in the data set. Number above each bar is the number of cases in that particular range of CAPE values.

3. For most tornado cases not satisfying guideline 1 or 2, proximity soundings were constructed by using proximity surface data representative of the inflow air and interpolating (for time and/or location) from the surrounding soundings both the boundary layer thermodynamic profiles and the standard level data above the boundary layer. The CAPE values for these tornado cases were derived from the constructed soundings. Soundings were constructed for three fourths (181 cases) of the cases utilized in the data set.

4. In a few instances, missing data or difficulties in interpolation resulted in potential cases being excluded from the data set.

The procedure for determining the CAPE for a case differs from that utilized to determine the mean shear and helicity values (see part 1). One of the reasons for the difference is that in determining CAPE, it was often necessary to consider the temperature profile through the depth of the entire troposphere. Also, the thermodynamic patterns (particularly for moisture) can be quite complicated in the boundary layer. These complications required that proximity soundings be constructed in most cases in order to arrive at a representative CAPE value.

2.2. *Surface Parcel Lifted Index (SPLI) Calculations*

An estimate of the instability may be obtained by computing SPLI values. For all of the tornado cases in which CAPE was successfully computed, SPLI values were also computed. The following method was employed to obtain SPLI values.

1. Surface temperature, dew point, and pressure values near the time and place of the event and representative of the air mass from which storm inflow was occurring were obtained.

2. A 500-mbar temperature for the time and over the place of event occurrence was obtained by interpolation from radiosonde constant level data.

3. By using a skew-T diagram the surface values for each event were combined to produce a measurement of the pseudo-adiabat which the surface parcel would follow if lifted to saturation. The difference between the temperature at which this adiabat crosses 500 mbar and the environmental 500-mbar temperature is the SPLI value.

3. Results

3.1. *Potential Buoyant Energy Distribution*

Figure 1 illustrates that the strong and violent tornadoes are associated with an extremely wide range of CAPE values. Values in the JDL data set range from 200 to 5300 J kg^{-1} with about two thirds (64%) of the cases exhibiting values between 1000 and 3000 J kg^{-1}. The data set displays seasonal and geographical differences in the values of CAPE associated with strong and violent tornado development. The cold season (November 1 to March 31) cases occur mostly in the eastern portions of the southern Plains and Gulf coastal region (see JDL) and exhibit CAPE values that are mostly weak to moderate (Figure 2). Ninety-five percent

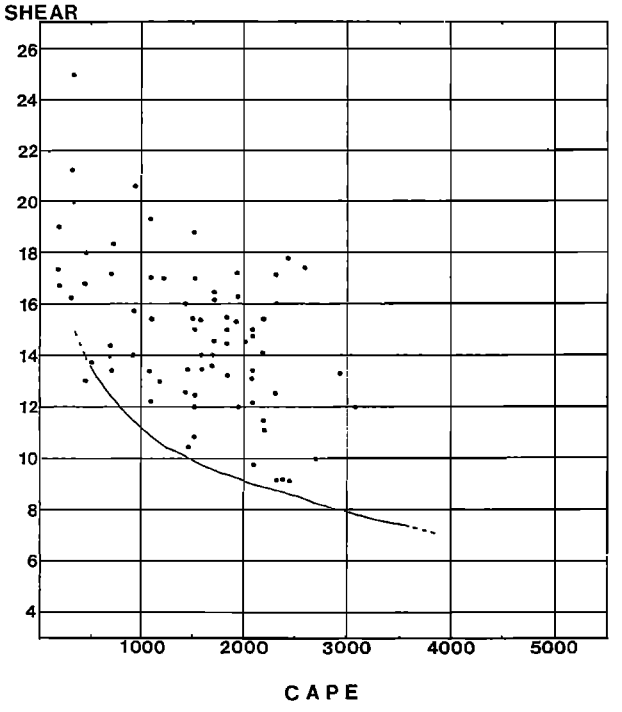

Fig. 2. Scatter diagram showing the relationship between convective available potential energy (CAPE) in joules per kilogram and 0-2-km AGL positive wind shear ($\times 10^{-3}$ s^{-1}) for the 75 cold season (November 1 to March 31) tornado cases. Solid curved line is a suggested lower limit of combined CAPE/low-level shear value that would support the development of strong or violent mesocyclone-induced tornadoes [after *Johns et al.*, 1990].

of the cold season cases are associated with CAPE values of less than 2500 J kg^{-1}.

Cases during the warm season (May 15 to August 31) generally occur farther west and north than the cold season cases (see JDL) and exhibit a wide range of CAPE values, from a weak 500 J kg^{-1} to a strong 5300 J kg^{-1} (Figure 3). The two cases exhibiting CAPE values of less than 1000 J kg^{-1} were associated with tropical cyclones. The low CAPE values in these cases agree with the findings of *McCaul* [1991]. The two cases associated with warm season derechos [*Johns and Hirt*, 1987] exhibit characteristically high CAPE values. Despite the wide range of values, note that over two thirds (68%) of the warm season cases are associated with CAPE values of 2500 J kg^{-1} or greater. This agrees with the findings of *Rasmussen and Wilhelmson* [1983].

Surface parcel lifted index (SPLI) values also suggest that strong and violent tornadoes are associated with a wide range of instability. Values in the JDL data set range from −1 to −14 (Figure 4). However, a large majority of the cases (72%) are associated with values from −5 to −10.

3.2. *Bulk Richardson Numbers*

Weisman and Klemp [1982, 1986] have shown that the type of storm that develops in a given environment is at least partially related to a Bulk Richardson Number (BRN) defined as

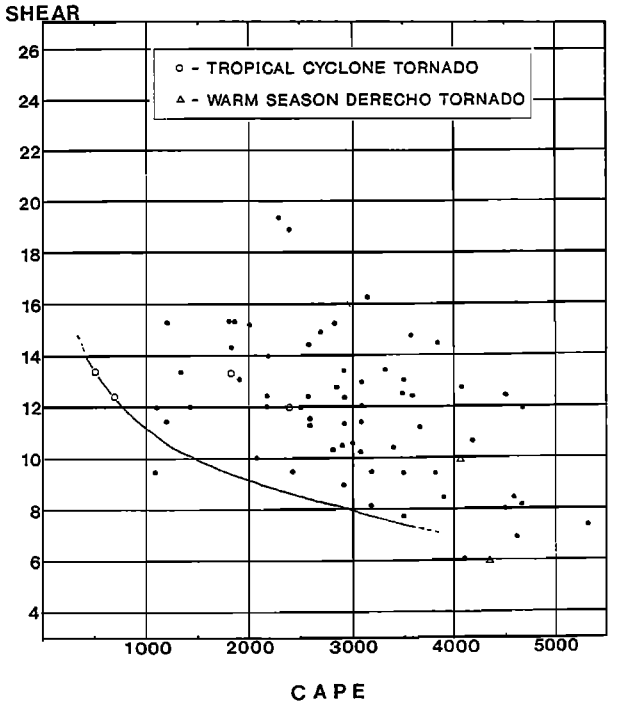

Fig. 3. As in Figure 2 except for the 69 warm season (May 15 to August 31) tornado cases. The open circles represent tornado cases associated with tropical cyclones. The open triangles represent tornado cases associated with warm season derechos [after *Johns et al.*, 1990].

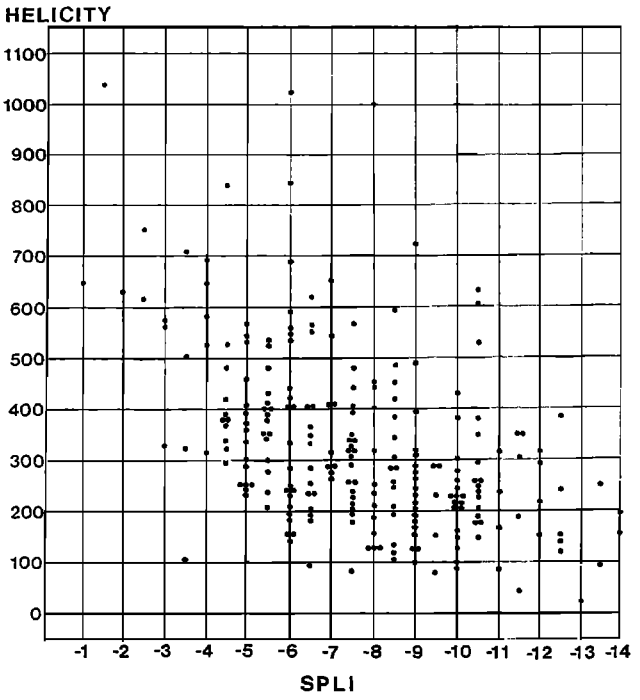

Fig. 4. Scatter diagram showing the relationship between surface parcel lifted index (SPLI) in degrees Celsius and 0- 2-km AGL helicity in $m^2\ s^{-2}$ utilizing the 20R85/30R75 storm motion assumption method for all 242 cases in the data set.

$$\mathrm{BRN} = \frac{B}{\frac{1}{2}U^2},$$

where B is the buoyant energy (CAPE) for a lifted parcel in the storm's environment, and U is a measure of the vertical wind shear through a relatively deep layer (0- 6-km AGL). Results from numerical modeling experiments and a limited number of storm observations have suggested that growth of supercells is confined to values of BRN between 10 and 40 [*Weisman and Klemp*, 1986].

Figure 5 illustrates the range of BRN values associated with the strong and violent tornadoes in the JDL data set. Almost one half (47%) of the BRN values are less than 8. The number of cases diminishes as the BRN values become larger, with most cases associated with values of less than 40 (94%). These results agree well with the findings of *Riley and Colquhoun* [1990], who also examined a large number of cases.

The question arises as to why there are so many cases with very low BRN values. The prevailing theory has been that in such an environment the very strong shear would inhibit the growth of the updraft, thus not allowing for a deep rotating convective column to develop and be sustained. One potential explanation for this apparent contradiction may lie with the nature of the BRN. As pointed out by *Weisman and Klemp* [1982] and *Lazarus and Droegemeier* [1990], the

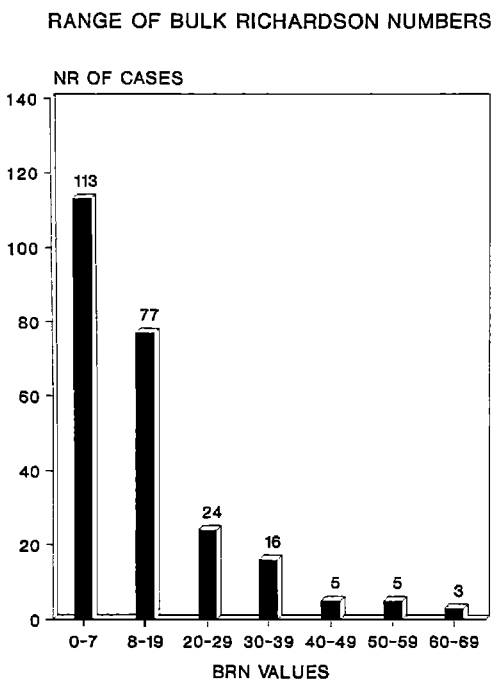

Fig. 5. Distribution of Bulk Richardson numbers [*Weisman and Klemp*, 1982] for all 242 strong and violent tornado cases.

BRN is a "bulk" measure of the ambient shear and does not account for detailed aspects of the wind profile, particularly low-level curvature. Modeling experiments [*Weisman and Klemp*, 1984; *Brooks and Wilhelmson*, 1990; *McCaul*, 1990] indicate that low-level curvature shear and storm-relative helicity interacting with the deeper tropospheric shear can enhance strongly the intensity of an updraft. McCaul's simulations of storms in the low-buoyancy environments of tropical cyclones indicate that shear-induced pressure forces [*Rotunno and Klemp*, 1982], related at least in part to the low-level curvature shear, can be up to 3 times as important as buoyancy in controlling updraft strength. Therefore it appears likely that in many situations where the BRN is a very low value, the low-level curvature shear plays a crucial role in helping to sustain a rotating convective column.

Although the above simulations suggest how a supercell might be maintained in a low BRN environment, there is still the question of initial development, or how an updraft can sustain itself in its earliest stages. Operational forecasting experience suggests a possible explanation for this question. The authors have observed cases where tornado-bearing supercells are associated with (or evolve from) complex convective structures, sometimes on a scale much larger than the supercell itself. Others have observed this type of storm structure (or evolution) also [e.g., *Nolen*, 1959; *Burgess and Curran*, 1985; *July*, 1990; *Moller et al.*, 1990; *Przybylinski et al.*, 1990]. Further, *Doswell et al.* [1990] have proposed that the "classic" isolated supercell is just one storm type in a broad range of storm types associated with supercell circulations. Examination of the radar imagery (low-elevation reflectivity data) associated with the 31 strong and violent tornado cases in the data subset described in part 1 supports the hypothesis of Doswell et al. Only 10 cases (32%) appear to be associated with "classic" isolated supercells, while the large majority of cases (68%) appear to be associated with a variety of multicellular systems including lines, spiral bands, clusters, and bow echoes. These results suggest that in strong and violent tornado situations, supercell circulations associated with complex multicellular convective structures are quite common.

Recall that the BRN is related to the type of storm structure that develops in a given situation [*Weisman and Klemp*, 1986]. The 10–40 range of BRN values that Weisman and Klemp have associated with supercell development applies to isolated convection (i.e., the "classic" isolated supercell). While an isolated supercell is not likely to develop in an environment with a very low BRN, the larger multicellular convective structures described in the previous paragraph can be initiated and sustained in such an environment by synoptic scale forcing (e.g., a squall line ahead of a cold front). Once developed, irregularities and differential movements in the storm outflow patterns [see *Doswell et al.*, 1990, Figure 4] may allow some updrafts to encounter enhanced inflow and develop rotation. Once rotation is established, the effect of shear-induced pressure forces (discussed earlier in this section) can help to sustain this rotation.

3.3. *CAPE and 0- 2-km AGL Positive Wind Shear Relationship*

While the BRN calculations involve the wind shear through a deep layer (0- 6-km AGL), recent interest has focused on the importance of both the shear and nature of the hodograph in the updraft inflow layer [e.g., *Davies*, 1989; *Davies-Jones et al.*, 1990; JDL]. JDL calculated 0- 2-km AGL positive wind shear for the purpose of indirectly estimating the rotational potential of the environmental wind field (i.e., the strength of the 0- 2-km AGL positive shear is related to the range of storm motions that would support supercell development).

To investigate the relationship of the low-level environmental shear to potential buoyant energy in strong and violent tornado situations, JDL constructed scatter diagrams. From Figures 2, 3, and 6 it is evident that there is a pattern to the combinations of 0- 2-km AGL PWS and CAPE associated with strong and violent tornadoes (Figure 6) and that there are seasonal variations in this pattern (Figures 2 and 3). For example, the cold season cases (Figure 2), which occur primarily from the eastern portion of the southern Plains into the Gulf coastal region, are generally associated with the combination of strong 0- 2-km AGL PWS values and weak to moderate CAPE values. Therefore the data points for cold season cases are concentrated in the upper left portion of the scatter diagram.

When considering all cases (Figure 6), the pattern of data

points suggests that progressively stronger 0- 2-km AGL PWS values are associated with strong and violent tornado development as the CAPE decreases. In a few cases where the PWS was very strong, greater than 16×10^{-3} s^{-1}, CAPE values as low as 200–300 J kg^{-1} were observed. At the other extreme, in situations where the CAPE was greater than 4000 J kg^{-1}, strong and violent tornadoes have been associated with PWS values as low as 6×10^{-3} s^{-1}. Despite the wide range of values there appears to be an optimum range of 0- 2-km AGL PWS values associated with strong and violent tornado development for any particular CAPE value. Further, JDL have shown that for violent tornadoes (F4 and F5 intensity) shear values are generally in the higher two thirds of any given optimum range.

3.4. *CAPE and Helicity Relationship*

Helicity has become an important parameter for evaluating the rotational potential of air in the storm inflow layer [e.g., *Davies-Jones et al.*, 1990]. To calculate storm-relative helicity a storm motion vector is needed. On the basis of the actual storm motions and the associated environmental conditions from a 31-case data subset, a method for assuming the storm motions from precursor conditions has been proposed (see part 1). This method assumes a storm motion of 20R85 (see part 1 for notation) for cases where the 0- 6-km AGL mean wind speeds are greater than 30 knots (15 m s^{-1}) and a motion of 30R75 for cases where the 0- 6-km AGL mean wind speeds are of lesser intensity. Although this method for assuming storm motions appears to be rather "crude," it does represent a refinement over applying a single assumed deviation, such as 30R75 [*Maddox*, 1976].

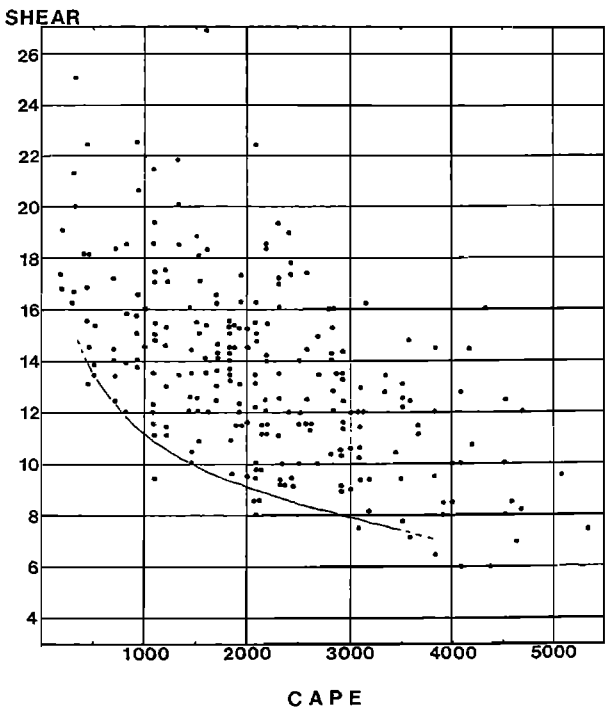

Fig. 6. As in Figure 2 except for all 242 cases in the data set [after *Johns et al.*, 1990].

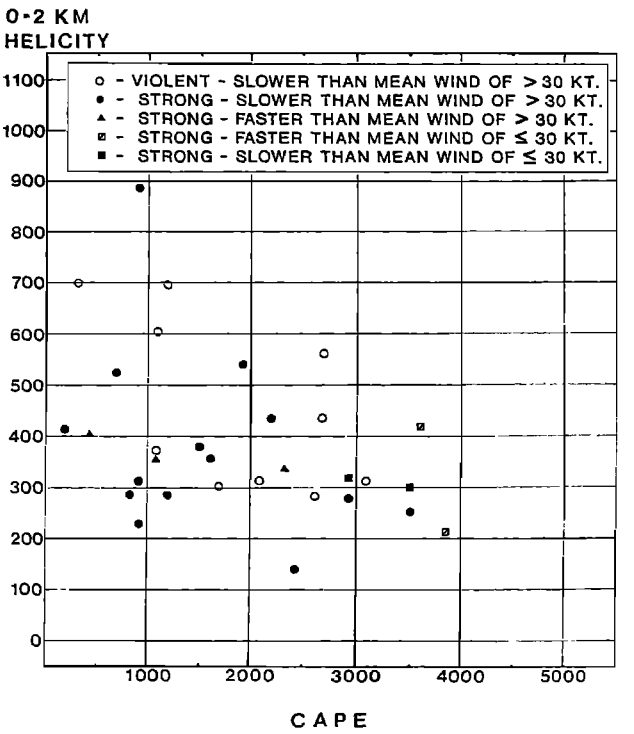

Fig. 7. Scatter diagram showing the combinations of convective available potential energy (CAPE) in joules per kilogram and 0- 2-km AGL helicity in m^2 s^{-2} utilizing observed storm motions for a 31-case data subset. Open circles represent violent tornadoes (F4-F5). All squares (solid and hatched) represent cases where the 0-6-km AGL mean wind speed is equal to or less than 30 knots (15 m s^{-1}). Triangles and hatched squares represent cases in which the associated supercell moves faster than the 0- 6-km AGL mean wind speed.

On the basis of the findings in part 1, the authors have chosen to construct and compare scatter diagrams displaying combinations of CAPE and helicity using the following criteria: (1) 0- 2-km AGL helicity using the observed storm motions for the 31-case data subset, (2) 0- 3-km AGL helicity using the observed storm motions for the 31-case data subset, (3) 0- 2-km AGL helicity using the 20R85/30R75 storm motion assumption method for the 242-case JDL data set, and (4) 0- 3-km AGL helicity using the 20R85/30R75 storm motion assumption method for the 242-case JDL data set.

Although the data sample is not large, the scatter diagram (Figure 7) depicting the combinations of 0- 2-km AGL helicity using observed storm motion and CAPE for the 31 subset cases displays a pattern that is qualitatively similar to the pattern for combinations of 0- 2-km AGL PWS and CAPE for the 242 JDL cases (Figure 6). There is a tendency for cases exhibiting strong values of low-level helicity to be

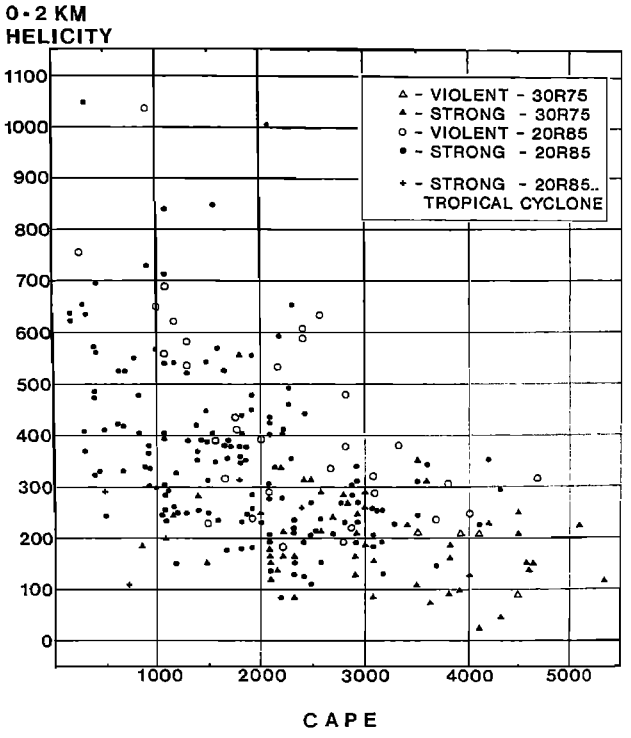

Fig. 8. Scatter diagram showing the combinations of convective available potential energy (CAPE) in joules per kilogram and 0- 2-km AGL helicity in $m^2\ s^{-2}$ utilizing the 20R85/30R75 storm motion assumptions for the 242 cases in the JDL data set. All triangles (open and solid) represent cases in which the assumed storm motion is 30R75, while the assumed storm motion for the remainder of the cases is 20R85. The open circles and open triangles represent violent tornadoes (F4-F5). The crosses represent cases associated with tropical cyclones.

associated with environments characterized by weak buoyancy, and vice versa. A scatter diagram (not shown) depicting 0- 3-km AGL helicity for the 31 subset cases is very similar to Figure 7.

In Figure 7, note that those cases in the subset which are associated with the weakest 0- 6-km AGL mean winds (equal to or less than 30 knots (15 m s^{-1}) and depicted as solid and hatched squares) are also associated with very high values of CAPE. This implies that supercell-induced strong and violent tornadoes occurring in a weak wind environment usually are associated with very strong to extreme instability.

When the 20R85/30R75 storm motion assumptions for computing helicity are applied to all 242 cases in the JDL data set, the resultant scatter diagram depicting combinations of 0- 2-km AGL helicity and CAPE (Figure 8) has a strong similarity to the one for 0- 2-km AGL PWS and CAPE (Figure 6). A progressively higher range of values for both helicity and PWS is associated with strong and violent tornado development as the CAPE decreases. However, the rate of change appears to be more gradual in the case of helicity and CAPE.

Since a number of researchers have used 0- 3-km AGL as the approximate inflow layer, a scatter diagram similar to Figure 8 has been prepared (not shown) with the only difference being that helicity has been computed using the 0- 3-km AGL layer. The scatter diagram patterns for both assumed inflow layers (0- 2-km and 0- 3-km AGL) are similar.

The four cases associated with tropical cyclones (indicated by crosses in Figure 8) tend to have relatively low values of both CAPE and helicity, resulting in the points residing in the lower left portion of the scatter diagram (one case in particular is far below the other points). The fact that tropical cyclone tornado cases normally are associated with low CAPE values is well documented [*McCaul*, 1991]. However, the reason for the accompanying low helicity values in Figure 8 is unclear. It may be related to the vertical distribution of helicity (helicity density) and the depth of the effective inflow layer [*McCaul*, 1991] (also see part 1). Also, there is a possibility that the motions of tornadic storms in tropical cyclone situations are estimated poorly by the storm motion assumptions utilized to compute helicity.

3.5. *SPLI and Helicity*

Figure 4 is a scatter diagram depicting the combinations of SPLI and 0- 2-km AGL helicity utilizing the 20R85/30R75 storm motion assumptions for all 242 cases in the JDL data set. The pattern is very similar to that for when CAPE is used as the instability parameter (Figure 8). The slightly greater scattering of points in Figure 4 is probably a result of the SPLI being a less precise method of estimating instability. Nevertheless, Figure 4 appears to have value for the operational forecaster who is computing SPLI values on an hourly basis and does not have access to the finer-incremented model forecasts of CAPE.

4. Discussion

From the JDL data set it has been determined that strong and violent tornadoes are associated with an extremely wide range of potential buoyant energy (CAPE) values. Most of the cases with low values of CAPE occur during the cooler months of the year and almost always are associated with dynamic weather systems and strong tropospheric wind fields (and wind shear). A few others with low CAPE values are associated with tropical cyclones. Both of these environments result in very low Bulk Richardson Number (BRN) values. As a result, when all strong and violent tornadoes are considered, almost half are associated with a BRN of less than 8. Until recently, the general perception has been that the BRN associated with supercell development should fit into a certain range, generally between 10 and 40. However, the results of this study (and the one by *Riley and Colquhoun* [1990]) suggest that while the BRN has utility in determining when the initiation of isolated supercells is possible, it is not a good discriminator for supercell development in general. This is particularly so for strong shear/low buoyancy situa-

tions (BRN from 0 to 8), which need to be recognized more widely as having potential for supercell-induced tornadoes.

The importance of low-level positive shear (PWS) and helicity in strong and violent tornado development has been discussed in part 1. When the combinations of these wind parameters with CAPE are considered, a definite pattern emerges. In cases where the values of CAPE are very high, the associated PWS values are usually relatively low. Generally higher values of PWS are associated with strong and violent tornado development as the CAPE decreases. At very low CAPE values, cases are associated with relatively high values of PWS. For any particular CAPE value there appears to be a range of PWS values that is optimum for strong and violent tornado development.

The relationship between CAPE and helicity in strong and violent tornado development is similar to that for CAPE and PWS. That is, generally higher values of helicity are associated with strong and violent tornadoes as the CAPE decreases. If it is assumed that most tornadoes in the data set are associated with supercells, then it can be stated that for any particular CAPE value there appears to be a range of helicity values that is optimum for inducing strong rotation and low-level mesocyclones in supercell storms (as suggested by *Lazarus and Droegemeier* [1990]).

The fact that there is considerable scatter on the PWS/CAPE and helicity/CAPE diagrams emphasizes that there are other factors involved in supercell-induced tornado development. One of these factors is the downdraft circulations affecting the supercell. It generally is accepted that if a supercell is to produce a mesocyclone-associated tornado, the development of a sufficiently strong rear flank downdraft (RFD) is necessary. The strength of the rear flank downdraft is dependent on conditions, particularly relative humidity, in its middle level source region.

Another factor also involves downdraft outflows, but usually on a larger scale. The intense downdraft and outflow that develops with some bow echoes affects storm motion, accelerating the storm structure. In some cases this results in the bow echo "experiencing" increased helicity, which may induce a supercell that is associated with the bow echo structure. Recall that in the 31-case data subset there were four cases associated with bow echoes that moved faster than the mean wind speed (from part 1). Note that the 20R85/30R75 storm motion assumptions used in constructing the helicity/CAPE diagram do not take this type of storm motion into account.

These two examples involve some effects of storm downdrafts. There are probably many more factors involved in supercell-induced tornado development (some of which are mentioned in part 1). This suggests that much additional work needs to be done toward understanding the processes that initiate and support storm rotation and mesocyclone-induced tornado development.

Acknowledgments. The authors especially appreciate the many hours of work volunteered by Grant Bean, Dave Higginbotham, and others of the NSSFC computer staff in assembling the massive data set for this study. The authors also wish to thank Bill Henry, NWSTC; Ken Howard, NSSL, ERL; Mike Ryba, WSO DDC; and Joe Schaefer, SSD, Central Region, NWS, for their help with this project and Deborah Haynes for helping with manuscript preparations.

References

Bothwell, P. D., Forecasting convection with the AFOS data analysis programs (ADAP-version 2.0), *NOAA Tech. Memo. NWS SR-122*, 91 pp., Natl. Weather Serv. S. Reg., Fort Worth, Tex., 1988.

Brooks, H. E., and R. B. Wilhelmson, The effects of low-level hodograph curvature on supercell structure, in *Preprints, 16th Conference on Severe Local Storms*, pp. 34–39, American Meteorological Society, Boston, Mass., 1990.

Burgess, D. W., and E. B. Curran, The relationship of storm type to environment in Oklahoma on 26 April 1984, in *Preprints, 14th Conference on Severe Local Storms*, pp. 208–211, American Meteorological Society, Boston, Mass., 1985.

Davies, J. M., On the use of shear magnitudes and hodographs in tornado forecasting, in *Preprints, 12th Conference on Weather Forecasting and Analysis*, pp. 219–224, American Meteorological Society, Boston, Mass., 1989.

Davies, J. M., and R. H. Johns, Some wind and instability parameters associated with strong and violent tornadoes, 1, Wind shear and helicity, this volume.

Davies-Jones, R. P., D. W. Burgess, and M. Foster, Test of helicity as a tornado forecast parameter, in *Preprints, 16th Conference on Severe Local Storms*, pp. 588–592, American Meteorological Society, Boston, Mass., 1990.

Doswell, C. A., III, J. T. Schaefer, D. W. McCann, T. W. Schlatter, and H. B. Wobus, Thermodynamic analysis procedures at the National Severe Storms Forecast Center, in *Preprints, 9th Conference on Weather Forecasting and Analysis*, pp. 304–309, American Meteorological Society, Boston, Mass., 1982.

Doswell, C. A., III, A. R. Moller, and R. W. Przybylinski, A unified set of conceptual models for variations on the supercell theme, in *Preprints, 16th Conference on Severe Local Storms*, pp. 40–45, American Meteorological Society, Boston, Mass., 1990.

Hales, J. E., Jr., and C. A. Doswell III, High resolution diagnosis of instability using hourly surface lifted parcel temperatures, in *Preprints, 12th Conference on Severe Local Storms*, pp. 172–175, American Meteorological Society, Boston, Mass., 1982.

Johns, R. H., and W. D. Hirt, Derechos: Widespread convectively induced windstorms, *Weather Forecasting*, *2*, 32–49, 1987.

Johns, R. H., J. M. Davies, and P. W. Leftwich, An examination of the relationship of 0-2 km AGL "positive" wind shear to potential buoyant energy in strong and violent tornado situations, in *Preprints, 16th Conference on Severe Local Storms*, pp. 593–598, American Meteorological Society, Boston, Mass., 1990.

July, M. J., Forcing factors in the violent tornado outbreak of May 5, 1989: A study in scale interaction, in *Preprints, 16th Conference on Severe Local Storms*, pp. 72–77, American Meteorological Society, Boston, Mass., 1990.

Lazarus, S. M., and K. K. Droegemeier, The influence of helicity on the stability and morphology of numerically simulated storms, in *Preprints, 16th Conference on Severe Local Storms*, pp. 269–274, American Meteorological Society, Boston, Mass., 1990.

Leftwich, P. W., Jr., and Wu X., An operational index of the potential for violent tornado development, in *Preprints, 15th Conference on Severe Local Storms*, pp. 472–475, American Meteorological Society, Boston, Mass., 1988.

Maddox, R. A., An evaluation of tornado proximity wind and stability data, *Mon. Weather Rev.*, *104*, 133–142, 1976.

McCaul, E. W., Jr., Simulations of convective storms in hurricane environments, in *Preprints, 16th Conference on Severe Local*

Storms, pp. 334–339, American Meteorological Society, Boston, Mass., 1990.

McCaul, E. W., Jr., Buoyancy and shear characteristics of hurricane-tornado environments, *Mon. Weather Rev.*, *119*, 1954–1978, 1991.

Miller, R. C., Notes on analysis and severe storms forecasting procedures of the Air Force Global Weather Central, *Tech. Rep. 200*, (rev.), 1972.

Moller, A. R., C. A. Doswell III, and R. Przybylinski, High-precipitation supercells: A perceptual model and documentation, in *Preprints, 16th Conference on Severe Local Storms*, pp. 52–57, American Meteorological Society, Boston, Mass., 1990.

Moncrieff, M. W., and J. S. A. Green, The propagation and transfer properties of steady convective overturning in shear, *Q. J. R. Meteorol. Soc.*, *98*, 336–352, 1972.

Nolen, R. H., A radar pattern associated with tornadoes, *Bull. Am. Meteorol. Soc.*, *40*, 277–279, 1959.

Przybylinski, R. W., S. Runnels, P. Spoden, and S. Summy, The Allendale, Illinois tornado—January 7, 1989—One type of an HP supercell, in *Preprints, 16th Conference on Severe Local Storms*, pp. 331–357, American Meteorological Society, Boston, Mass., 1990.

Rasmussen, E. N., and R. B. Wilhelmson, Relationships between storm characteristics and 1200 GMT hodographs, low level shear, and stability, in *Preprints, 13th Conference on Severe Local Storms*, pp. J5–J8, American Meteorological Society, Boston, Mass., 1983.

Riley, P. A., and J. R. Colquhoun, Thermodynamic and wind related variables in the environment of United States tornadoes and their relationship to tornado intensity, in *Preprints, 16th Conference on Severe Local Storms*, pp. 599–602, American Meteorological Society, Boston, Mass., 1990.

Rotunno, R., and J. B. Klemp, The influence of the shear-induced pressure gradient on thunderstorm motion, *Mon. Weather Rev.*, *110*, 136–151, 1982.

Weisman, M. L., and J. B. Klemp, The dependence of numerically simulated convective storms on vertical wind shear and buoyancy, *Mon. Weather Rev.*, *110*, 504–520, 1982.

Weisman, M. L., and J. B. Klemp, The structure and classification of numerically simulated convective storms in directionally varying wind shears, *Mon. Weather Rev.*, *112*, 2479–2498, 1984.

Weisman, M. L., and J. B. Klemp, Characteristics of isolated convective storms, in *Mesoscale Meteorology and Forecasting*, edited by P. S. Ray, pp. 331–358, American Meteorological Society, Boston, Mass., 1986.